DRAG-FREE CONTROL DESIGN INCLUDING ATTITUDE TRANSITION FOR THE STEP MISSION

Patrick Chapman[a], Dr-Ing. Peter Zentgraf[b], Dr. Yusuf Jafry[c]
[a]Astrium Ltd; [b]Astrium GmbH; [c]ESTEC;
Astrium Ltd, EU73, Gunnels Wood Road, Stevenage, Herts, SG1 2AS, England
Tel: +44 1438 773709, Fax: +44 1438 778913, E-mail: patrick.chapman@astrium-space.com

Abstract

The proposed Satellite Test of the Equivalence Principle (STEP) Mission aims to test the Equivalence Principle with higher accuracy than previously obtained by ground based experiments. STEP was recently proposed as a joint NASA/ESA mission, with ESA providing the service module (SVM); this would be a standard LEOSTAR design.

The mission uses low thrust proportional thrusters for either 3-DOF or 6-DOF control in different phases. During the attitude acquisition sequence the thrusters can be used as pure torque actuators. In the later science mode they are used for 6-DOF (force and torque) control as part of the drag-free attitude control system (DFACS). The paper presents simple designs for both these control modes.

Initial coarse attitude acquisition is by a standard LEOSTAR mode. The fine acquisition mode which follows is specific to STEP. This mode must damp initial body rates, perform a small slew, and control during a wheel de-spin, all using very low control torques.

For the DFACS mode rotational and translational control laws are designed as multiple single-input-single output (SISO) loops using simple proportional-integral-derivative PID type controllers. Six-degree-of-freedom simulations demonstrate that during the period of scientific measurement of the STEP mission, the thrust coming from the boil-off helium which is used to provide cooling for the superconducting measurement devices is sufficient to maintain an acceleration below the requirement, thereby confirming previous predictions [5] from simplified models.

Introduction

The weak equivalence principle (EP) essentially asserts that gravitational mass for any body is the same as its inertial mass irrespective of the composition and the mass of the bodies. As a result of this all bodies will fall at the same acceleration in the same gravitational field.

The STEP spacecraft is to test the validity or otherwise of the weak equivalence principle by dropping a pair of masses of differing composition and mass in the Earth's gravitational field but in order to increase the sensitivity of the experiment to drop them in earth orbit. The experiment uses pairs of hollow cylindrical test-masses, nested one inside the other. Each mass is constrained to essentially one degree-of-freedom by use of a super-conducting cylindrical 'bearing'. The STEP spacecraft consists of four pairs of almost freely-suspended test masses inside a drag free controlled spacecraft. This paper essentially covers the design and performance of the control laws for the attitude transition and the DFACS modes; it is a summary of [1].

The basic idea to detect a possible violation of the EP is to compare the behaviour of two test masses exposed to gravity in an environment where the DFACS has suppressed external disturbances. In order to achieve the required accuracy the controller must keep the *inertial* acceleration (system "i" in fig. 1) at the test mass position below $3 \times 10^{-14}\,\mathrm{m/s^2}$ (RMS, across measurement bandwidth (MBW) of 10^{-5} Hz) in the presence of any disturbance acting on the spacecraft and the test masses. The SQUID magnetometers [2] provide a common-mode signal (the "average" position of the two test masses w.r.t. the spacecraft, x_r and y_r in fig. 1) which is used for control.

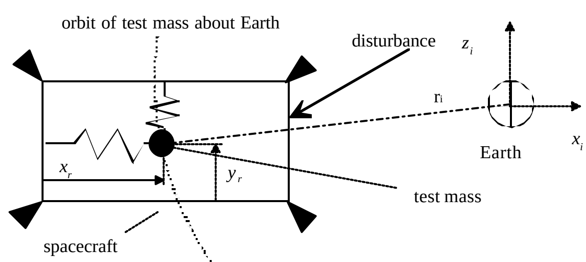

Figure 1: Schematic View of the Drag-Free Control Problem. The single test mass is an idealized representation of the common-mode readout from a differential pair

In the normal science mode the spacecraft slowly rotates about its Z axis, at a spin rate of the order of a few times orbit rate. The spin is normal to the orbit plane, and provides the modulation of the EP signal, which occurs at $\omega_{EP} = \omega_{spin} - \omega_{orbit}$. Different spin rates will be used during the mission to repeat the experiment at different frequencies.

Disturbance Environment

STEP will fly in a sun-synchronous dawn-dusk low eccentricity, low Earth orbit (LEO). There are several perturbing effects that act on the control system in this environment, the dominant ones being aerodynamic drag, gravity gradient and magnetic disturbance torque. The combination of the spacecraft's spin and orbit rate causes both the drag force and drag torque to be modulated in a spacecraft referenced frame at exactly the science signal (EP) frequency (shown in figure 3). Any disturbance acting at EP frequency on the test masses propagates at a reduced level into the differential mode that provides the science signal, mimicking an EP violation. It is thus essential that the control system introduces a significant disturbance attenuation at the EP frequency, and to demonstrate this the drag must be accurately modelled. A major part of the study [1] was to investigate if drag-free performance can be met at altitudes as low as 400 km, with realistic assumptions about sensor and actuator dynamics and noise properties.

Atmospheric density in LEO varies on many time scales. In the long term the density is correlated with the 11 year solar cycle, having its minimum value at solar minimum. The 6 month mission must lie near to solar minimum, in order that the limited thrust from the helium boil off can negate the air drag. The planned launch is 2005, which is near the next solar minimum. For simulation purposes the MSIS 86 (Mass spectrometer – incoherent scatter) model has been used to model the density, using predicted solar activity typical of past solar minima.

MSIS predicts density variations at up to a few times orbit rate. At higher frequencies (up to 0.1 Hz) there are hypothesized to be local atmospheric effects beyond the resolution of the MSIS model, due to localized density variations [5]. Fig. 2 shows the modelled air density measured at the spacecraft position over two orbits, including both the MSIS results and an additive high frequency "noise" to represent the hypothesized local effects.

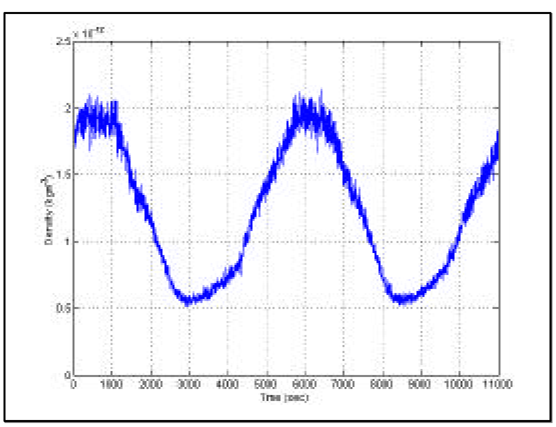

Figure 2: Variation of air density at 400 km for predicted estimate of activity at solar minimum

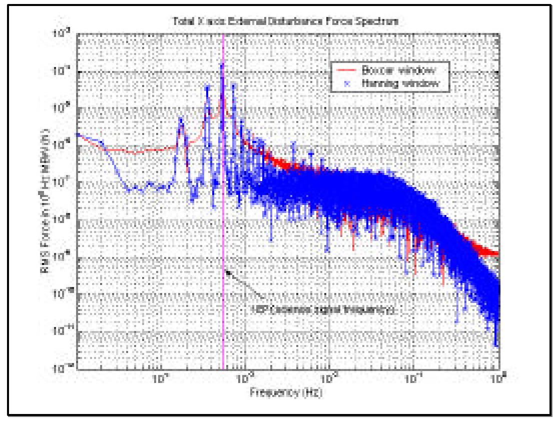

Figure 3: External force spectrum, for a spacecraft axis lying in the orbit plane

A gravity model is required for orbit propagation and for the detailed modelling of the performance of the test masses due to the gravity gradient terms, due to the relative separation of spacecraft centre of mass and the test masses. The mathematical model is implemented by the use of a series of Legendre polynomials, using the GEM (Goddard Earth Model). Small geographic surface features below the GEM resolution (such as mountains) cause acceleration levels which in open loop would be expected to be significant, but in closed loop these will be attenuated far below the science requirement level and so are not necessary to model. The order of model used is high enough to include effects at the critical EP frequency.

The final part of the environment model is magnetic disturbance torque. This depends on the Earth's magnetic field and on the assumed spacecraft magnetic dipole of [5 5 5] Am^2. The Earth field is modelled using the 10^{th} order International Geomagnetic Reference Field with the latest (year 2000) values extrapolated to 2005.

Spacecraft Modelling

The STEP configuration consists of a payload module (PLM) and a polyhedral service module (SVM). The PLM consits of a cylindrical dewar containing the payload, which is cryogenically cooled with liquid helium. Helium gas boiled-off the dewar is used as the propellant for a set of 16 cold gas proportional thrusters. The SVM is topped-off by a wider circular solar array which permanently shadows the rest of the spacecraft from direct sunlight. It contains magnetorquers (MTQ) as actuators.

The spacecraft's shape dictates that the spin is about the axis of minimum inertia, and so active 3-axis attitude control is used to maintain the attitude, according to a reference profile generated in the DFACS. An

Autonomous Star Tracker (AST) is located on the base of the dewar, aligned along –Z (the anti-sun orbit normal direction), to provide absolute attitude data.

MTQ's are required for certain mission phases (acquisition and safe mode), and so are potentially available to the PLM as actuators. However the preference is to not use these during science mode if possible, to avoid possible magnetic interaction with the payload. It also simplifies interfaces between the payload computer (which hosts the fine transition mode and the DFACS) and SVM (which hosts acquisition and safe mode) if MTQ are not used by modes hosted in the PLM.

Various aspects of the spacecraft are modelled in order that realistic disturbances can be simulated. The simulation includes force and torque disturbances due to air drag, gravity gradient and solar radiation, and also magnetic disturbance torque.

The test masses are modelled as simple spring-mass-damper systems, located at a finite distance from the C of G. Each test mass has a sensitive axis (either X or Y, representing the cylindrical bearing axis) with low spring constant and two relatively insensitive axes (representing the cylinder radial axes) with higher spring constants. Common-mode position measurements are output at 10 Hz with standard deviation of σ=1 nm for the sensitive axis, and with σ=3.2 nm for the 'insensitive' axis.

Thruster Modulation

Thruster Configuration

As a baseline the thruster configuration from [3] was used. This design consists of 4 groups of 4 thrusters (T_1, T_2,...T_{16}) with each group separated by 90 deg around Z in the XY plane. Eight of the thrusters lie in the XY plane (at α=20 deg to +/- X or Y), and eight lie at β=20 deg to +/- Z. The 8 thrusters in the XY plane provide most of the drag force compensation, and are modulated as the spacecraft rotates (fig. 4).

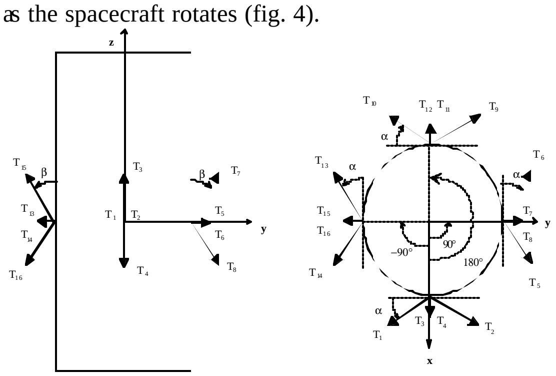

Figure 4: Thruster Configuration [3]

The original thruster configuration from [3] was modified for this study in two aspects: Firstly, the thruster direction angle β is chosen to be 38 deg such that the thrusters fire in a sufficient large angle off the structure to be compliant with the plume impingement requirement (this avoids plumes on the wide solar array "lid" on +Z, added since [3]). This reduces the force capacity in Z-direction to the benefit in of the force capacity in X/Y-direction. Secondly, in order to increase the torque capacity the thrusters are placed on struts.

Thruster Modulation Algorithms

The demanded forces and torques from the controller are now realized by firing the 16 thrusters. To find a suitable set of 16 individual thrust values satisfying the controller demand is complicated by the fact that two conditions must be satisfied at any time:

Condition 1: The total mass flow of all thrusters must be 1.5 mg/s

Condition 2: Each thruster must have a minimum mass flow of 10% of the average mass flow

The problem can be posed as a linear optimization problem:

$$\underline{\text{Minimize}}\ S x_i \text{ while solving } Ax = b \text{ for } \underline{x} \le x_i \quad (1)$$

where x_i is the (unknown) mass flow of thruster i, A is the (known) 6x16 thruster distribution matrix, b the (known) 6x1 controller demand vector and $\underline{x}$ is the minimum mass flow of each thruster. The problem (1) can uniquely be solved using the simplex method (i.e. with Matlab-function "linprog" [4]). If the solution of (1), x^*, has the property that $\Sigma\ x_i^*$ exceeds the value of 1.5 mg/s of condition 1 then this particular control demand cannot be generated without violating condition 1; the demands must be reduced until the conditions 1 and 2 are met. On the other hand, if $\Sigma\ x_i^*$ lowers the value of 1.5 mg/s then the solution x^* of (1) is scaled up by adding a null space vector (firing all thrusters with the same amount) such that the sum of mass flow of all thrusters is 1.5 mg/s. Unfortunately, this technique requires too much computation time (in a Matlab/Simulink model 0.17s for one particular controller demand on a 600 MHz PC) for a practical real-time environment. Therefore, the solution of (1) was merely used as a reference to evaluate faster modulation algorithms.

Two "fast" modulation algorithms have been investigated; they are both about 50 times faster than Matlab-function "linprog"[4]. A recursive modulation algorithm proposed in [3] was compared with a modulator not requiring an iteration ("non-iterative pseudo-inverse modulator") which is presented next.

The idea of this modulator is as follows: For a particular force/torque demand, the scalar product of the force/thrust vector versus the thrust direction/thrust torque vector is computed for each thruster. Those thrusters having a large contribution are identified and those who have little contribution are considered to be useless for this particular demand and are set to minimum mass flow rate. Then, the necessary thrust is computed by pseudo-inversion of the thruster matrix consisting of the remaining thrusters. It is "hoped" by that means, that the satisfaction of the minimum mass flow constraint is easier performed by eliminating the "useless" thrusters. The process of pseudo-inverting is repeated for several promising thruster candidates. Finally, the best solution is taken. The idea is best explained by example. Imagine a two dimensional thruster set as shown in fig. 5 where the unit force of the single thrusters are drawn in bold print. Given a specific force demand f, thrusters 3 and 4 have a positive scalar product (see "s_3" in fig. 5) whereas thrusters 1 and 2 cannot contribute directly (negative scalar product) to yield the demanded force.

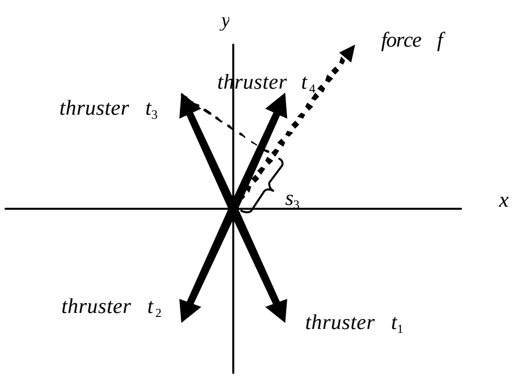

Figure 5: Principle of Non-Iterative Pseudo-Inverse Modulator

Therefore, they are set to minimum thrust t_{min} and for thrusters 3 and 4 any linear combination of αt_3 and βt_3 using arbitrary scalars α and β is allowed to solve the demand. This leads to solve a system of linear equations for the unknowns α and β:

$$a \ t_3 + b \ t_4 = f - t_{\min} t_2 - t_{\min} t_1 \qquad (2)$$

The principle can directly be generalized in three dimensional space and in addition with torque demands to be satisfied. The advantage of this modulator is that no iterations are involved.

The performance of the modulator from [3] and of the non-iterative pseudo-inverse modulator were evaluated in the following way. Typical force/torque demands of the STEP-controller (with and without support of MTQ's) were fed into the modulators and violations of conditions 1 and 2 were evaluated by the factor how much the demand had to be lowered compared to the original demand such that conditions 1 and 2 could finally be satisfied. Both modulators showed similar performance but were not able to recover thruster demands without use of MTQ. Therefore, on top of each thruster modulation algorithm the thrust demands were balanced using the full null space [1]. This did not increase computation time but improved the performance such that MTQ's were no longer necessary.

Attitude Transition Mode

The initial off-launcher coarse attitude acquisition is via a standard LEOSTAR mode, ASH (acquisition and safe hold) [2]. ASH acquires to the approximate attitude required for STEP's science mode using MAG sensors, MTQ actuators and a fixed momentum bias provided by a reaction wheel aligned along Z. ASH is hosted in the SVM, which has direct interfaces to the MAG, MTQ and wheel.

A transition mode is needed to remove the residual attitude/rate errors and de-spin the wheel. For simple interfaces between the PLM and SVM, a mode design is preferred with a clean separation of roles between the two modules, and hence a design is sought which can be hosted on the PLM (which controls the thrusters), without using the MTQ (controlled by the SVM), and which has simple requirements for the wheel de-spin.

In the worst case the initial attitude error from ASH may be several degrees, and hence the transition mode must perform a small slew. The attitude dynamics of STEP are dominated by the momentum bias of the still spinning reaction wheel, hence it is interesting to ask which order is "best" overall for the slew and de-spin manoeuvres, bearing in mind that the thruster control torques are no more than ~2 mNm. If the de-spin is done first, the wheel's gyroscopic rigidity is removed, making it easier to slew. However if the slew is done first, it reduces the likelihood that the Earth horizon will enter the AST FoV, causing degradation or loss of attitude data. Both options may take a few orbits due to the small torques available.

A pulsed torque precession method has been investigated, similar to those used on traditional spin stabilised spacecraft, for slewing whilst the wheel is spinning. For a fraction of each spin a constant torque is delivered, causing the momentum vector to precess. After precessing through a half-cone a second application of torque kills the motion. This method suffers from the problem that for STEP the control torque provided during the pulsing phases is only slightly higher than the maximum possible disturbance torque, which acts continuously during the thrusting and coast phases (this is in contrast to most spinning spacecraft which benefit from much larger thrusters). This can cause the precession path to be very distorted, compared with the idealised, disturbance-free simple coning motion. For this reason, precession by torque impulses has been discarded, and a closed loop controller has been designed.

The solution chosen for the X and Y axes is a non-linear rate-limited proportional derivative (RLPD) control design, shown as fig. 6 below. RLPD combines within a simple control structure damping of the initial body rates and slewing at a chosen fixed rate to the reference attitude (in the RL phase), followed by settling at the reference attitude (in PD phase). The slew rate is chosen to be low enough that the wheel's gyroscopic torque can be offset by the thrusters. The slew rate can be "high" (~8"/s) if the wheel is de-spun at mode entry, but must be less if de-spin occurs during or after the slew. The Z (spin) axis is controlled by a simple rate controller, with the rate reference ramped slowly to the nominal value. For all axes the AST is used to provide attitude data, which is differenced to generate angular rates.

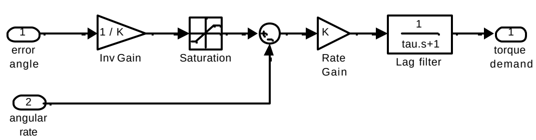

Figure 6: RLPD control law used on X and Y axes

The overall duration of slew time and wheel de-spin can be used as an optimisation cost function. If the wheel is rapidly de-spun (requiring a large Z torque from the thrusters) whilst slewing, then there is little X/Y thruster torque available for slewing. If the spacecraft slews and de-spins the wheel simultaneously, then the slew rate must be low, due to the wheel stiffness, but the final attitude may be acquired quickly. This is summarised by fig. 7 below, showing total manoeuvre time for different options, factoring in the usable torque envelope.

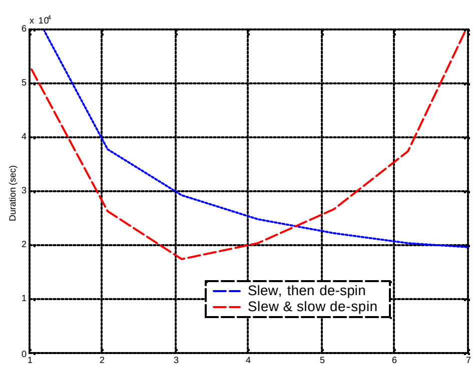

Figure 7: Optimised acquisition duration

If the best slew rate is chosen for each option, then slewing with simultaneous de-spin is roughly as fast as slewing and then de-spinning, but the later option acquires the nominal attitude three times quicker, and is therefore preferred.

The chosen scenario is therefore to slew to the required attitude and then de-spin the wheel. This makes the best use of the limited control torque available. Closed loop simulations have been run of this design (fig. 8), which show that the Z axis can be slewed at 7 arcsec/sec using thruster torque, whilst the wheel is still spinning.

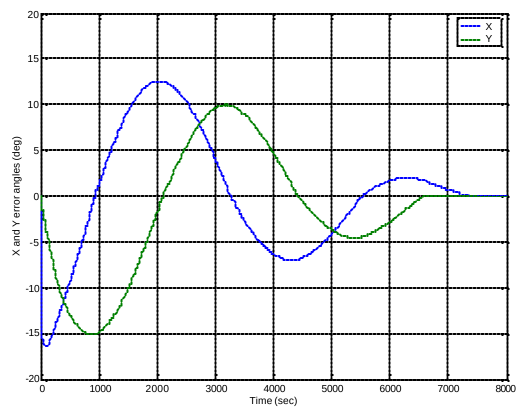

Figure 8: Error angles during simulated fine attitude acquisition, using thruster only torque

After a slow de-spin the wheel is held fixed in place by stiction torque. During the science mode it behaves as a rigid part of the spacecraft.

DFACS Design

The controller is represented at high level by Fig. 9 below, showing the DFACS (hosted on the payload computer), and its interfaces to outside equipment.

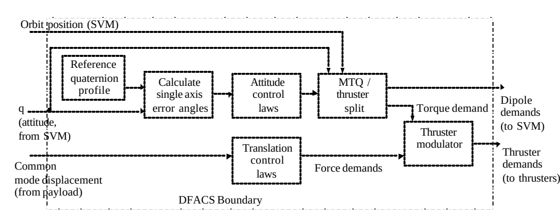

Figure 9: DFACS Control System Block Diagram

Orbital position (provided by the SVM) is used to drive an on-board magnetic field model, but this is only required if the MTQ are used. (This interface is only required if MTQ use is needed by the DFACS). The DFACS interface requirements are seen to be simplified if MTQ use is avoided.

The study investigated if successive loop-closure using simple SISO designs is feasible, motivated by the fact that the motions are so small that cross-couplings should be negligible w.r.t. controller design. Therefore the attitude quaternion is manipulated to provide Euler error angles which are input into three single-axis attitude control laws. Similarly common-mode position errors are used to drive three single-axis translation control laws. To avoid unstable interactions between the attitude and translation axes, the bandwidths of these controllers have been separated.

A constraint for a linear controller design is that the noise levels of the force and torque demands must be below the saturation limits of the actuators. The cold gas thrusters are modulated about a mean thrust level of only 0.12 mN, and can saturate for spacecraft axis force demands significantly greater than this. The controllers were chosen to have gains as high as possible subject to the constraint that the force and torque demands (in spacecraft axes) were limited to $\sigma_{Force} <\sim 10^{-4}$ N and $\sigma_{Torque} <\sim 10^{-4}$ Nm.

Choosing stable controllers which meet the constraints above determines the performance at frequencies well above the science signal frequency. At EP frequency a number of options were investigated to give very high attenuation of external disturbances in order to provide very low acceleration in the region of the MBW. Figure 10 below shows the transfer functions from force disturbance and measurement noise to spacecraft acceleration, using a SISO linear model of a translation loop.

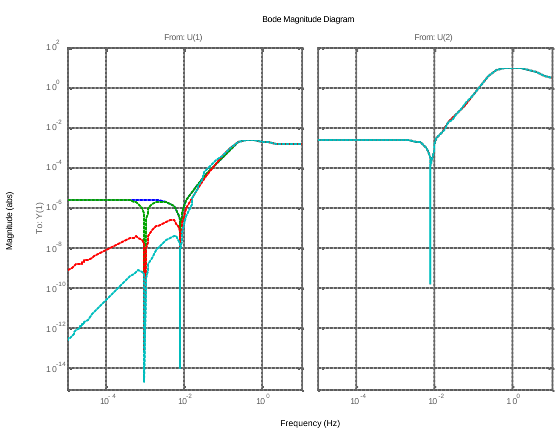

Figure 10: Force (left), Measurement Noise (right) to acceleration gains

The notch feature at f=0.008 Hz is caused by the test mass spring constant (value for an insensitive axis).

The left hand plot shows controllers with incremental improvements (curves from top to bottom):

1 Simple lead compensator
2 Addition of a notch filter in series. This attenuates the main drag disturbance at f_{EP} (here f_{EP} = 1 mHz).
3 Addition of a 1st order integrator in parallel with the lead filter.
4 Addition of a 2nd order integrator in parallel with the lead filter.

Each of these additions improves the disturbance force rejection at low frequency. However it is also seen (in the right hand plot) that in all these cases the low (near EP) frequency dependency on measurement noise is unchanged. The low frequency asymptote is found to be a function of the plant model only, and not the controller values. Hence the ultimate level of performance is when disturbance forces are reduced so low that the total acceleration is dominated by the effects of measurement noise only.

Notch filtering at the EP frequency can be used to attenuate the main drag force to very low levels, but only across a narrow frequency range (if a wide frequency range is sought then the notch also reduces the phase margin). Second order notch filters were investigated, and were found to provide acceptable attenuation (in combination with the integral action described above) without causing a serious erosion of phase margin. It was also found that the narrow width of the notch was acceptable in the presence of "de-tuning" effects from errors in knowledge or variability of the spin rate and orbital period.

DFACS Simulation Results

A number of test cases were run under simplified conditions (e.g. constant drag force) to give confidence that low acceleration levels could be simulated, and that the results agreed with theory. After this more detailed simulations including the MSIS, GEM10 and IGRF models were run, with all noise sources included.

Simulation results showed that it was possible to maintain control at 400 km during solar minimum conditions with the use of thrusters only (i.e. without using MTQ for supplementary torque).

The acceleration spectrum which results shows that translation control has performance at EP near the limits set by the test mass position measurement noise. This limit is:

$$\text{RMS accel. in } \Delta f \text{ bandwidth} = \sigma_{Meas}\, \omega_n^2 \left(2T\, \Delta f \right)^{1/2} = 1.1 \times 10^{-14}\ \text{m/s}^2 \qquad (3)$$

for the less sensitive radial axes of the test mass (T is the measurement sample time, ω_n is the natural frequency of the spring force of the test mass).

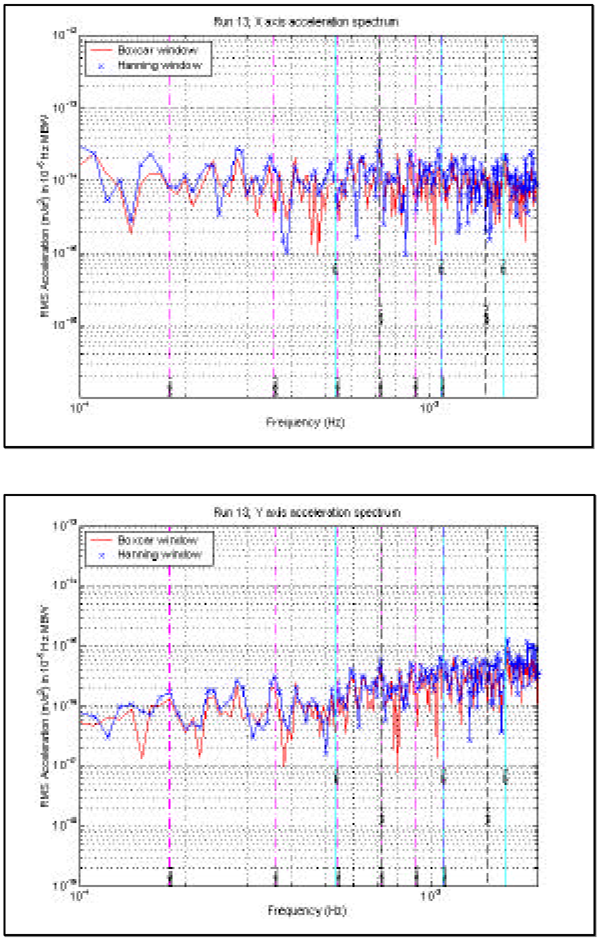

Figure 11: Simulated Acceleration Spectrum Results for a radial axis (top) and sensitive axis (bottom)

Figure 11 depicts the RMS acceleration at the test mass equilibrium position (fig. 1) within frequency sampling bins of width Δf=MBW. This resolution requires generating 10^5 sec duration simulations, which take several hours of run-time on a PC. In this example f_{EP} = 0.54 mHz (= 3 times orbit rate).

The X (radial) axis spectrum above shows a flat low frequency spectrum, as expected for a system limited by the measurement noise (from fig. 4). The Z radial axis is very similar to X. Boxcar and Hanning windows were used to generate the spectra, to give increased confidence in the frequency domain results obtained. The two radial axes show an acceleration noise level very close to the theoretical value, indicating that drag and gravity gradient disturbances have been attenuated so well that the overall performance is measurement noise-limited. The sensitive (Y) axis acceleration at EP is ~100 times better than X, due mainly to its lower ω_n. Its spectrum is also less flat than X, due to a spin dynamics cross coupling effect from measurement noise on X.

The performance on the radial axes is only a factor of ~2 better than the requirement, at the limit set by the measurement noise characteristics

Conclusions

The attitude transition phase between ASH and DFACS can be bridged using the thrusters as the sole torque actuators, with simple interfaces between the NASA PLM and the ESA SVM.

The STEP drag-free acceleration requirement can be met at 400 km altitude using helium thrusters alone, i.e. without magnetotorquers, due to a new and fast modulator (patent pending, [6]) which expands the usable thruster force/torque envelope compared with previous work [3]. Detailed time domain simulations confirm earlier predictions [5] that a simple SISO control design can achieve the required level of low-frequency acceleration performance, which is limited by the measurement noise process only, and has no control law dependency.

Acknowledgement:

This work was performed under ESA/ESTEC contract 15139/01/NL/HB.

References

1. Chapman, P., Zentgraf, P., *Drag-Free Control Analysis and Algorithm Design for the STEP Mission Feasibility Study*, Technical Report, GNC/TNO/STEP/2033, Issue 2, September 2002

2. NASA/ESA, STEP Phase A Interim Report, Draft issue, JPL, July 2001

3. Jin, H., Wiktor, P., DeBra, D., An optimal thruster configuration design and evaluation for Quick STEP, *13th IFAC Symposium Automatic Control in Aerospace – Aerospace Control '94*, September 12-16, 1994.

4. Coleman, T. F., Branch, M. A., Grace, A., *Optimization Toolbox - User's Guide Matlab*, pp. 4-91 - 4-97, The MathWorks Inc., 1999

5. Jafry Y, *Journal of Classical and Quantum Gravity*. vol. 13, Number 11A, pp. A179-A184, 1996

6. UK Patent Application No. 0203950.1 filed on 20 February 2002